Dissipative friction dynamics within the density-functional based tight-binding scheme

Eric Michoulier, Didier Lemoine, Fernand Spiegelman, Sven Nave, Mathias Rapacioli

Eur. Phys. J. Spec. Top.
https://doi.org/10.1140/epjs/s11734-023-00937-y

THE EUROPEAN PHYSICAL JOURNAL SPECIAL TOPICS

Regular Article

Dissipative friction dynamics within the density-functional based tight-binding scheme

Eric Michoulier[1,a], Didier Lemoine[1,b], Fernand Spiegelman[2,c], Sven Nave[1,3,d], and Mathias Rapacioli[2,e]

[1] Laboratoire Collisions Agrégats Réactivité (LCAR/FeRMI), Université Toulouse III - Paul Sabatier and CNRS, 118 Route de Narbonne, F-31062 Toulouse, France
[2] Laboratoire de Chimie et Physique Quantiques (LCPQ/FeRMI), Université Toulouse III - Paul Sabatier and CNRS, 118 Route de Narbonne, F-31062 Toulouse, France
[3] Institut des Sciences Moléculaires d'Orsay, CNRS and Université Paris-Saclay, Rue André Rivière, Bât. 520, F-91405 Paris Cedex, France

Received 11 January 2023 / Accepted 2 July 2023

Abstract The accurate description of an atom or molecule colliding with a metal surface remains challenging. Several strategies have been performed over the past decades to include in a Langevin dynamics the energy transfer related to electron–hole pair excitations in a phenomenological way through a friction contribution. We report the adaptation of two schemes previously developed in the literature to couple the electronic friction dynamics with the density-functional based tight-binding (DFTB) approach. The first scheme relies on an electronic isotropic friction coefficient determined from the local electronic density (local density friction approximation or LDFA). In the second one, a tensorial friction is generated from the non-adiabatic couplings of the ground electronic state with the single electron–hole excitations (electron tensor friction approximation or ETFA). New DFTB parameterization provides potential energy curves in good agreement with first-principle density-functional theory (DFT) energy calculations for selected pathways of hydrogen atom adsorbing onto the (100) silver surface or penetrating subsurface. Preliminary DFTB/Langevin dynamics simulations are presented for hydrogen atom scattering from the (100) silver surface and energy loss timescales are characterized.

1 Introduction

Collisions of atoms and molecules with surfaces are of interest in several domains ranging from fundamental physics, nanosciences and nanotechnologies, up to astrochemistry (formation of cosmic dusts and nanograins in the interstellar medium) or environmental sciences (formation of pollutants in the atmosphere). The case of metallic substrates is particular since they present a continuum of virtual electronic states, with vanishing energetic separations from the occupied levels. Hence, non-adiabatic energy transfer from the projectile towards the conduction bands of the metal can occur at very weak energy, inducing dissipation of the collision energy through population of excited electronic states. This is known in surface physics as dissipation due to electron–hole excitation.

In principle, theoretical schemes do exist to treat non-adiabatic excited states dynamics, such as the Tully Trajectory Surface Hopping scheme [43] or the mean field Ehrenfest scheme. However, the energy balance can be seriously biased in the Ehrenfest scheme, while the reach of statistical convergence in the Tully scheme meets a bottleneck in the special case of metals, due to the high density of electronic states. Moreover, the use of explicit schemes is often restricted to model Hamiltonians and cannot yet be combined with first-principle-based methods such as density-functional theory (DFT) and time-dependent (TD) DFT in the case of metallic systems. Alternatively, methods have been developed to incorporate electronic dissipation within Born–Oppenheimer ground-state molecular dynamics, via the use of the Langevin stochastic dynamics and the addition of a friction term [5, 7, 14, 17, 18, 24, 32]. Then, the electron–hole pair excitations are accounted

[a] e-mail: eric.michoulier@gmail.com
[b] e-mail: didier.lemoine@irsamc.ups-tlse.fr
[c] e-mail: fernand.spiegelman@irsamc.ups-tlse.fr
[d] e-mail: sven.nave@universite-paris-saclay.fr
[e] e-mail: mathias.rapacioli@irsamc.ups-tlse.fr (corresponding author)

Published online: 27 July 2023

for as a dissipative bath acting onto the nuclei dynamics either using an isotropic [7, 14, 24] or a tensorial friction term [5, 17, 18, 32] in the Langevin equation. DFT dynamical studies of collision with surfaces are generally conducted with periodic boundary conditions, defining slabs to describe the surface. However, simulations with DFT can still be limited in terms of simulation times, statistics of trajectories with various initial conditions or the limited size of the supercells. Actually, friction simulations are often finally achieved via potentials fitted to reproduce first-principle DFT energy behavior on selected collisional pathways [20, 31]. Such potentials may not necessarily account for the full electronic structure calculations. The density-functional based tight-binding (DFTB) scheme [15, 16, 39] is an approximate version of DFT, and is one to three orders of magnitudes more efficient in term of computational speedup. Thus, it can be considered as an interesting alternative to DFT for extended systems [9, 40], keeping approximate but explicit electronic structure.

In the present work, we illustrate the adaptation of the friction formalism to the DFTB framework and its implementation within the deMonNano code [1]. Benchmarks and preliminary applications to the collision of H with a (100) silver surface are reported. This system was chosen according to the experimental studies of Kolovos-Vellianitis and Küppers [25] who started to characterize the competition of the adsorption and of the subsurface insertion channels through measuring thermal desorption spectra (TDS) as a function of either H or D exposure. It is noteworthy that subsurface insertion was not evidenced with Ag(111), whereas the relevant TDS peak becomes much larger than that from surface sites at the highest exposures with Ag(100). Furthermore, at these high exposures, a surface reconstruction could be evidenced for H and yet not for D, which then represents a huge isotopic effect. The detailed dynamics of both hydrogen subsurface insertion (absorption) and resurfacing (desorption) has not yet been studied theoretically for Ag(100). This would require both an accurate and an efficient description of tens of scattering or diffusing hydrogen atoms as well as of hundreds of vibrating and/or relaxing silver atoms at the least, in order to reproduce either the TDS spectra or the surface reconstruction reasonably well. There is a need to characterize abstraction reactions, namely molecular hydrogen recombinations between an incoming hydrogen atom and an adsorbed one. Their computed cross-sections could be compared with the experimental estimates for H reacting with D/Ag(100) and D/Ag(111) as a function of coverage [25]. The present work represents the first step to these aims.

2 Coupling friction dynamics with DFTB

The self-consistent-charge (SCC) formulation of DFTB was developed by Elstner et al [12] as an extension of the original DFTB framework [36, 39]. It is based on the main following approximations: (i) the Kohn–Sham DFT total energy functional is expanded up to the 2nd order around a reference electronic density n_0, the second-order terms being expressed as a function of the atomic charges, (ii) molecular orbitals (MO) ϕ_i are expressed on a minimal valence atomic basis χ_μ and (iii) 3-center atomic integrals are neglected. The final expression for the DFTB total energy reads

$$E_0 = \sum_{A<B} V_{AB}^{rep} + \sum_{i,\mu,\nu} n_i c_{\mu i} H^0_{\mu\nu} c_{\nu i} + \frac{1}{2} \sum_{A,B} \Delta q_A \gamma_{AB} \Delta q_B \tag{1}$$

where n_i is the occupation number of orbital ϕ_i, μ and ν are the Kohn–Sham atomic orbital indices, Δq_A is the Mulliken charge of atom A. V_{AB}^{rep} is an atomic pair repulsive contribution between atoms A and B and $H^0_{\mu\nu}$ is the matrix element expressed in the atomic basis of the Kohn–Sham operator taken at the reference electronic density n_0. $c_{\mu i}$ are Kohn–Sham MO coefficients and γ_{AB} describes the Coulomb interaction between spherically symmetric charge distributions centered on atoms A and B with a short range exchange-correlation contribution. The total energy E_0 is searched following the self-consistent procedure as proposed by Elstner et al. [12] solving the secular equation for the MO coefficients vectors C_i and orbital energies ϵ_i:

$$HC_i = \epsilon_i S C_i \tag{2}$$

where S and $H = H^0 + H^1(q)$ are the overlap and DFTB operator matrices in the atomic orbital basis. H^0 is the band Hamiltonian and $H^1(q)$ is the second-order charge-dependent operator. In the standard parameterization recipe, the elements of the Hamiltonian and overlap matrices expressed in the atomic basis are computed from atomic and diatomic DFT calculations and the repulsive potential is fitted from diatomic dissociation curves. The γ_{AB} matrix elements are computed from Hubbard parameters. The periodic formulation of DFTB was reported by several groups [4, 26, 37, 39].

The Langevin dynamics with electronic friction stems from the substitution of a non-adiabatic dynamics with the full excited electronic degrees by a Langevin dynamics in the ground state [2, 42]. In the quasi-static or Markovian limit, the motion is described by the following Langevin equation

$$M\ddot{\mathbf{R}}_A = -\nabla_{\mathbf{R}} E_0 - \mathbf{F}_A + \boldsymbol{R}(t, T_e) \tag{3}$$

where E_0 is the electronic ground-state adiabatic potential energy. The forces in the equation involve (i) the energy gradient usual in conservative classical molecular dynamics, (ii) a dissipative force $\mathbf{F}_A$ acting on atom A and (iii) a $\boldsymbol{R}(t, T_e)$ a random fluctuating force at time t and electronic temperature T_e ensuring detailed balance and the fluctuation-dissipation theorem.

The dissipation forces can be determined by two different approaches. In the local density friction approximation (LDFA) [7, 11, 19, 21, 24, 31, 38],

$$\mathbf{F}_A = \eta \dot{\mathbf{R}}_A \tag{4}$$

where η is a scalar friction coefficient computed from the electron density of the metals. In the ETFA scheme developed by Head-Gordon and Tully [18, 32] or Forsblom and Persson [14], the friction term is a tensor (Λ_{AB}) determined explicitly from the non-adiabatic couplings of the ground state with the excited electronic states.

$$\mathbf{F}_A = \sum_B \Lambda_{AB} \dot{\mathbf{R}}_\mathbf{B} \tag{5}$$

In the following, we consider the coupling of the DFTB scheme with both ETFA and LDFA approaches.

We start with the tensorial approach, following the formulation of Maurer et al. [32]. In the ETFA approach, the Λ_{AB} matrix in Eq. 5 is computed considering explicitly the hole–particule excitations and the non-adiabatic coupling of the occupied orbitals with the virtual ones [14, 18, 32]. In the low temperature and weak coupling limit and in the quasi-static approximation, the anisotropic friction tensor can be estimated as

$$\Lambda_{AB} = \pi\hbar \sum_{ik} \mathbf{\Gamma}^A_{ki}\mathbf{\Gamma}^B_{ki}(\epsilon_i - \epsilon_k)^2 \tilde{\delta}(\epsilon_k - \epsilon_F)\tilde{\delta}(\epsilon_F - \epsilon_i) \tag{6}$$

In the adaptation to the DFTB scheme, the sum runs over the DFTB occupied (ϵ_i) and unoccupied (ϵ_k) energy levels and ϵ_F is the Fermi level calculated as the medium level between the HOMO and LUMO orbitals. $\tilde{\delta}$ is a broadened Dirac function

$$\tilde{\delta}(\epsilon_j - \epsilon_i) \simeq \frac{\sqrt{2}}{\sqrt{\pi}\sigma} \frac{exp[-(\epsilon_j - \epsilon_i)^2/(2\sigma^2)]}{[1 - erf(\epsilon_j - \epsilon_i)]} \tag{7}$$

Following the work of Maurer et al. [32], the broadening σ was set at 0.6 eV. $\mathbf{\Gamma}^A_{ki}$ is the non-adiabatic coupling between orbitals ϕ_i and ϕ_k:

$$\begin{aligned}\mathbf{\Gamma}^A_{ki} &= < \phi_k | \boldsymbol{\nabla}_{\mathbf{R}_A} | \phi_i > \\ &= \sum_{\mu,\nu} \frac{c_{\mu k}(\boldsymbol{\nabla}_{\mathbf{R}_A} H^0_{\mu\nu} - \epsilon_i \langle \boldsymbol{\nabla}_{\mathbf{R}_A} \chi_\mu | \chi_\nu \rangle - \epsilon_j \langle \chi_\mu | \boldsymbol{\nabla}_{\mathbf{R}_A} \chi_\nu \rangle) c_{\nu i}}{\epsilon_i - \epsilon_k}\end{aligned} \tag{8}$$

We used the approximations detailed in the work of Maurer et al. [32], namely averaging the left and right derivatives of the atomic overlaps and assuming that, on average, occupied and unoccupied states are symmetric about the Fermi level. Within these conditions $\mathbf{\Gamma}^A_{ki}$ can be simplified as

$$\mathbf{\Gamma}^A_{ki} = \sum_{\mu,\nu} \frac{c_{\mu k}(\boldsymbol{\nabla}_{\mathbf{R}_A} H^0_{\mu\nu} - \epsilon_F \boldsymbol{\nabla}_{\mathbf{R}_A} S_{\mu\nu}) c_{\nu i}}{\epsilon_i - \epsilon_k} \tag{9}$$

In practice, the Γ^A_{ki} elements are calculated using the coefficients, energies and DFTB operator of a non-scc calculation (i.e., neglecting the second-order H^1 contribution in Eq. 2). However, in the Langevin Eq. 3, the energy derivatives $\nabla_\mathbf{R} E_0$ used in the dynamics were determined within the full SCC scheme (i.e., using the H^1 contribution in Eq. 2).

We now consider the alternative LDFA scheme [7, 14, 21, 24, 31], in which the friction coefficient is isotropic and depends on the electronic density of the metal at the position of the considered atom. The densities for the whole system (slab + projectile) at a given position of the projectile were determined via the DFTB orbital coefficients and expressions of the atomic basis (hsd files from dftb.org website). Finally the friction coefficient η was determined as a function of the Wigner–Seitz radius $r_s[\mathbf{r}(t)] = [3n(\mathbf{r}(t))/4\pi]^{\frac{1}{3}}$, a quantity commonly used to describe the electron gas of the metal. In practice, η is a decreasing function of r_s and was fitted from Fig. 1 of [24]. The ETFA scheme has been directly implemented in an additional module to the deMonNano code [1] making use of its recently implemented periodic version [37]. The LDFA friction coefficient is computed by external routines from the electronic densities provided by the deMonNano code.

3 DFTB parameterization from DFT/PBE calculations

In order to optimize the DFTB parameterization, we started to determine reference data from DFT first-principle spin-polarized total energy calculations using the DFT-based Vienna ab initio simulation package (VASP), developed at the Institut für Materialphysik of the Universität Wien [27–29]. This approach uses a plane-wave basis set, and the non-local exchange-correlation effects are treated within the generalized gradient approximation (GGA) using the Perdew–Burke–Ernzerhof (PBE) exchange-correlation functional [34, 35]. The interactions between the ionic cores and the electrons are described by fully non-local optimized projector augmented-wave (PAW) pseudopotentials [8, 30]. Spin-polarized calculations have been performed with the plane-wave expansion truncated at 400 eV. An asymmetric slab supercell with periodic boundary conditions (PBC) has been employed to model the system as an infinite slab. In this study, the substrate consists of five layers with a square 2×2 unit cell, corresponding to four metal atoms per layer and an adsorbate coverage of 1/4 ML (monolayer corresponding to one hydrogen atom per supercell). A vacuum space of nine layers has been used to separate the substrate and its repeatable images. All DFT calculations

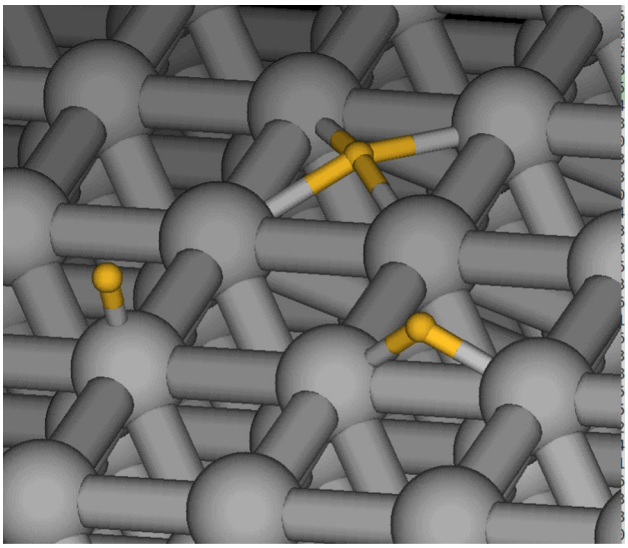

Fig. 1 Top, Hollow and Bridge positions of H above the Ag(100) surface (from left to right, H atoms in yellow)

were performed at the equilibrium lattice constant of 4.163 Å, as found from the bulk geometry optimization in VASP using the same DFT/PBE scheme. This is slightly larger than the experimental value 4.0867 Å [10] and the results of previous DFT/GGA calculations in the range 4.059−4.159 Å [6, 23]. The Brillouin zone is sampled by a 10×10×1 Γ-centered grid of k points.

There are three high-symmetry H-adsorption sites on the Ag(100) surface, hereafter labeled as Bridge, Hollow and Top (see Fig. 1). The (100) surface unit cell is squared with four Ag atoms at the corners. The Top site is that with H above a single Ag atom, the Bridge site lies above the middle of a side and the Hollow site slightly above the middle of the unit cell. Vertical paths for H incident above the high-symmetry adsorption sites as well as three non-activated paths (i.e., with no potential barrier to overcome) for H subsurface insertion were explored. The three non-activated paths are the vertical path passing through the Bridge sites and two 45° incidence paths, the first one aiming at the Hollow site and the second aiming at the surface site located halfway between a Hollow and a neighboring Top site. First, the Ag atoms were fixed at their equilibrium positions. Second, full (x, y, z) relaxation of Ag atoms was allowed, except for the two bottom-most layers that are constrained to remain fixed in order to represent the bulk, plus (x, y) relaxation of H in the case of non-vertical paths for a given z position of H. The computed H-adsorption binding energies and equilibrium positions above the surface plane are negligibly modified upon relaxation of Ag atoms. This yields binding energies of −1.94, −1.96, and −1.47 eV for the Bridge, Hollow and Top sites, respectively, and positions of 1.11, 0.46, 1.77 Å above the surface for the same respective sites. In contrast, interaction energies can be strongly decreased upon relaxation of Ag atoms when H is in the surface plane or subsurface. For example, the energy along the path for an incident H through the Bridge site shows oscillations with an energy maximum for H near the Bridge site at each layer, the first maximum at the surface layer being decreased by 0.78 eV upon relaxation. Similarly, for a 45° incidence path passing through Hollow sites, the maxima are located nearly halfway between two layers and the first one under the surface is decreased by 1.14 eV upon relaxation. The subsurface absorption sites are found under the Bridge site, nearly halfway between two layers, with binding energies of −1.47 and −1.59 eV, for the first and second ones, respectively. Those results are in very good agreement, energy and position differences being less than 0.1 eV and 0.1 Å, respectively, with those listed in Table 1 of [13], that is for the Bridge and subsurface sites.

The Ag–Ag DFTB parameters are those adapted in our previous work [33] on Ag clusters and nanoparticles and which were shown to provide fairly accurate results on structural and binding properties from the dimer up to the bulk. The resulting DFTB bulk lattice constant is 4.067 Å, thus slightly smaller than the DFT/PBE value above. In the case of Ag–H interaction, the available parameters taken from the dftb.org website (so-called Hybrid parameterization [41]) significantly overshoot the binding energy of the AgH molecule (D_e=3.50 eV vs 2.39 eV experimentally). Therefore, we modified the hopping and overlap integrals. A distance shift (0.78 Bohr) and a unique scaling multiplier (0.8327) was applied to both hopping and overlap integrals. Similarly, the repulsion was reparameterized so that the SCC-DFTB energies along several selected paths fitted the above DFT/PBE calculated energies with an equivalent slab supercell (2×2×5), the same k-points and the same level of relaxation. These calculations were performed with the DFTB+ package [4].

Figure 2 shows for the optimal parameters the comparison between the SCC-DFTB and the DFT/PBE results along three paths: the two vertical paths for H incident above either the Hollow (top) or the Bridge (center) site, with no Ag relaxation, and the minimum energy path (bottom) obtained upon full relaxation of the Ag atoms and upon relaxing H along x and y. The minimum energy path corresponds to a 45° incidence path aiming at the surface site located halfway between the Hollow and Top sites. The first point on the left side corresponds to H probing the repulsion of the Ag atom directly below the surface Hollow site (upper panel) or H at the Bridge (center panel) or Hollow (lower panel) site in the fourth Ag layer. In all cases, the DFTB results are quite consistent with the DFT/PBE data. In addition, this parameterization provides an Ag–H potential curve (equilibrium distance R_e=1.59 Å, dissociation energy D_e=2.76 eV) energetically closer to available ab initio calculations [3, 44, 45] (R_e in the range 1.57−1.61 Å, D_e in the range 2.36−2.63 eV) or experimental data [22] (R_e=1.618, D_e=2.39 eV) than the "Hybrid" parameterization mentioned above (R_e=1.62 Å, D_e=3.50 eV).

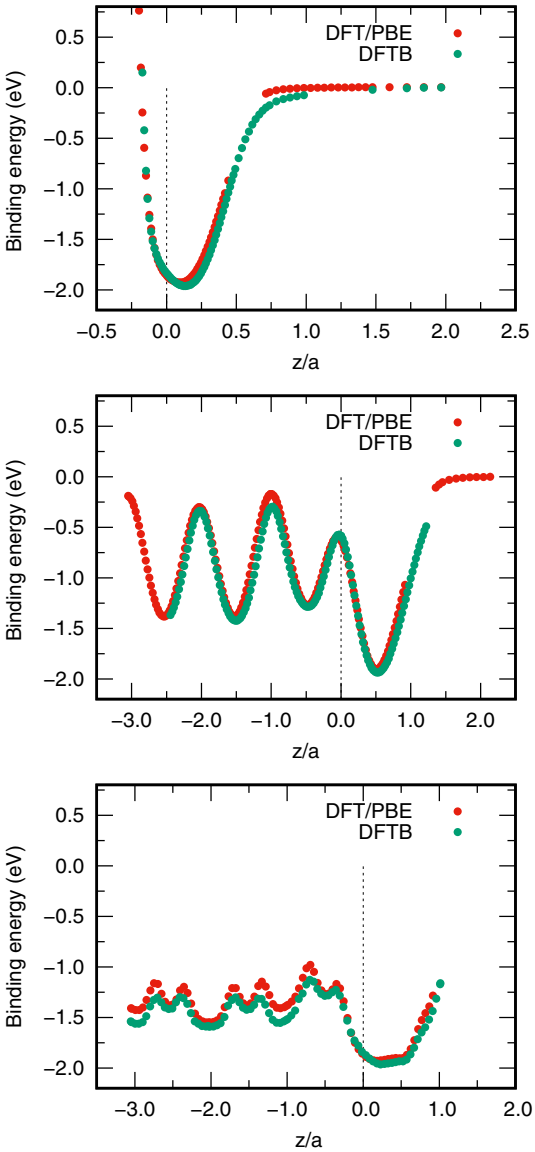

Fig. 2 Comparison between DFTB and DFT/PBE energies along three selected paths: vertical paths for H incident above the Hollow (upper panel) and Bridge (center panel) sites, with no Ag relaxation, and the minimum energy path (lower panel) for a 45° incident H with full relaxation (see text). z/a is the z coordinate relative to the respective DFT/PBE or DFTB lattice constant, a, with the origin at the surface (vertical dashed lines)

4 DFTB/Langevin dynamics application

The DFTB calculations have been conducted with PBC conditions and restriction to the Γ point of the Brillouin zone. The silver metal was modeled via a slab. The supercell included 6×6 atoms per layer and 5 layers, i.e., 180 atoms and is shown in Figs. 3 and 4. Figure 5 shows the components Λ_{xx}, Λ_{yy} and Λ_{zz} of the tensorial friction along the vertical path above the Hollow site. Consistently with the symmetry along this path, the tensor is diagonal in the main slab axes and the components Λ_{xx}, Λ_{yy} are found to be equal while Λ_{zz} is a bit different.

The top plot of Fig. 6 shows the comparison of the average of the tensorial components (the third of the trace) and the value of the LDFA scalar friction along the vertical path above the Hollow site. The bottom plot shows the energy variation along the same path (note that the binding energy is slightly smaller than that obtained from the above fitting procedure, due to the use of a larger supercell and of the Γ-point approximation). The good agreement observed in the top panel can be expected for the Ag noble metal, having a closed d electronic shell, which induces a small density of states at the Fermi level and consequently a low electron–hole pair excitation efficiency from H scattering dynamics, as speculated by Kolovos-Vellianitis and Küppers [25] who indirectly evidenced a notably weak friction regime in their experiments. In such a regime LDFA proves to be a good approximation. This fair correspondence allows us to demonstrate the consistency of our DFTB implementation and furthermore constitutes the first theoretical study that confirms the above-mentioned speculation [25]. Note that conversely, a strong departure from LDFA was found by Askerka et al. [5] in the case of H with Pd(100). From their Fig. 1, the LDFA scalar friction can be calculated to be 3.9, 3.9, 3.5 and 2.9 times larger than the isotropic average of the tensorial friction at the Hollow, Bridge and Top adsorption sites and at the subsurface absorption site, respectively. The greatest deviation among their studied cases occurring at the Hollow and Bridge sites, it is thus relevant to illustrate the comparison for Ag(100) with the vertical path above the Hollow site.

We now report a molecular dynamics study of H scattering from Ag(100) under normal incidence. All atoms were left to move freely except for the two bottom-most

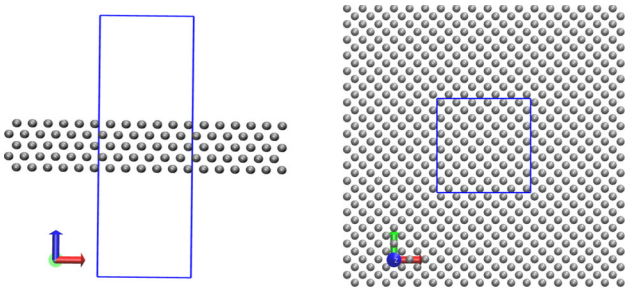

Fig. 3 Ag slab with periodic box drawn. Left: side view. Right: top view

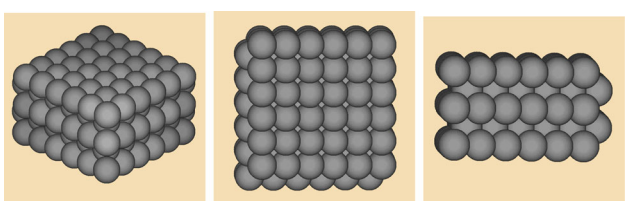

Fig. 4 3D views of the Ag slab unit cell

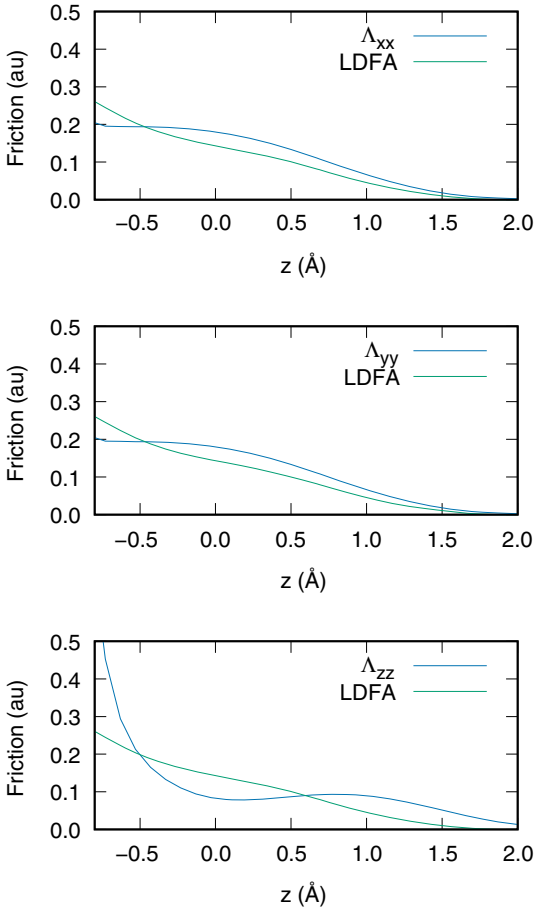

Fig. 5 LDFA friction coefficient (green) and diagonal components (Λ_{xx}, Λ_{yy}, Λ_{zz}) (blue) of the tensorial friction along the vertical path above the Hollow site. The origin of the z coordinate is at the surface

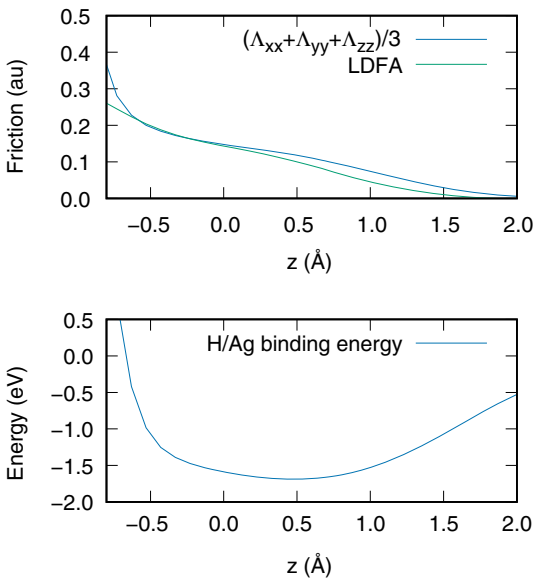

Fig. 6 Top: comparison of the LDFA friction and of the isotropic average of the tensorial friction along the vertical path above the Hollow site. Bottom: energy profile along the same path. The origin of the z coordinate is at the surface

Ag layers that are constrained to remain fixed in order to represent the bulk. The initial energy of hydrogen was set at 0.2 eV and the temperature to zero. The results were compiled over 64 trajectories, sampling randomly the initial position of H within an irreducible triangular area which apexes lie in a plane parallel to the surface above the Bridge, Hollow and Top sites. The resulting dynamics can be rather complex, often showing multiple bounces. Figure 7 displays selected trajectories illustrating the three possible outcomes for H scattering from Ag(100), i.e., adsorption, absorption and backscattering. Compilation over the 64 trajectories yields the following results: 25 % of the trajectories lead to the backscattering of H to the gas phase, 50 % to adsorption and 25 % to absorption, most often between the surface and the second layer.

Energy transfer of the projectile to the surface is obviously a crucial quantity to report. Figure 8 shows the energy loss for two characteristic trajectories, the first one leading to direct absorption and the second one to adsorption. Both trajectories are characterized by a rapid decrease extending up to 1.5 ns. However, while the energy loss in the adsorption regime, involving only surface scattering, is fairly well represented by a single exponential decrease $\exp(-t/\tau)$ with $\tau \approx 420$ fs, a double exponential fitting with different characteristic times, respectively 195 and 410 fs, is needed to correctly reproduce the energy loss evolution in the absorption regime, involving both surface and subsurface scattering and thus two distinct timescales.

5 Conclusion

Using a modified set of DFTB parameters for the AgH interaction, we were able to reproduce several energy pathways obtained from plane-wave first-principles DFT calculations. We have adapted the tensorial and LDFA friction formalism to the DFTB framework, which gives access to large supercells and to dynamical simulations. A check was made for the symmetry of the tensorial components with respect to x–y for the normal incidence pathway crossing the Hollow site. In addition, the isotropic average of the tensorial friction was found to be in good agreement with the isotropic LDFA friction term, which can be expected for the Ag noble metal, having a closed d electronic shell, which induces a small density of states at the Fermi level and consequently a low electron–hole pair excitation efficiency from H scattering dynamics, as speculated by Kolovos-Vellianitis and Küppers [25] who indirectly evidenced a notably weak friction regime in their experiments. In such a regime LDFA proves to be a good approximation. This fair correspondence validates the consistency of our DFTB implementation. It is, to our knowledge, the first theoretical study that confirms the above-mentioned speculation [25]. Normal incidence molecular dynamics within the tensorial Langevin scheme for H scattering from Ag(100) with 0.2 eV energy reveals complex trajectories at and below

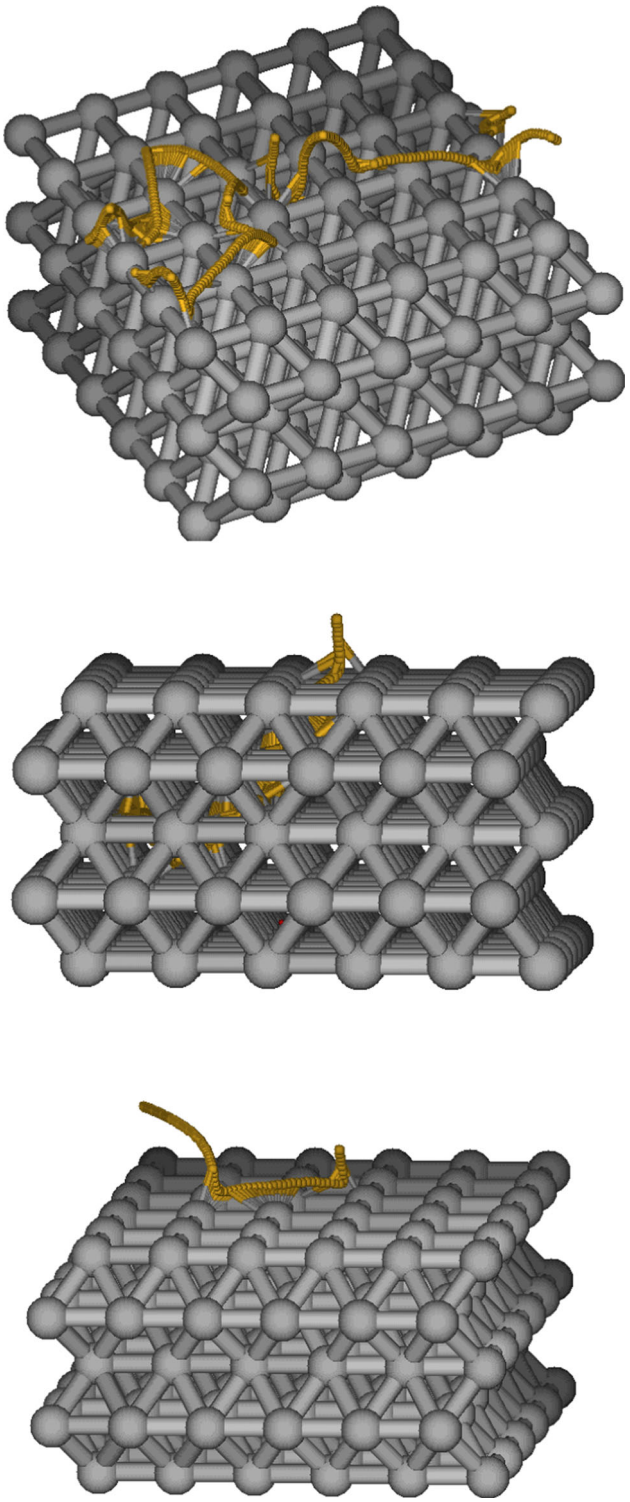

Fig. 7 Selected trajectories illustrating the three possible outcomes for H scattering from Ag(100) under normal incidence above the Hollow site: adsorption (top), absorption (center) and backscattering (bottom)

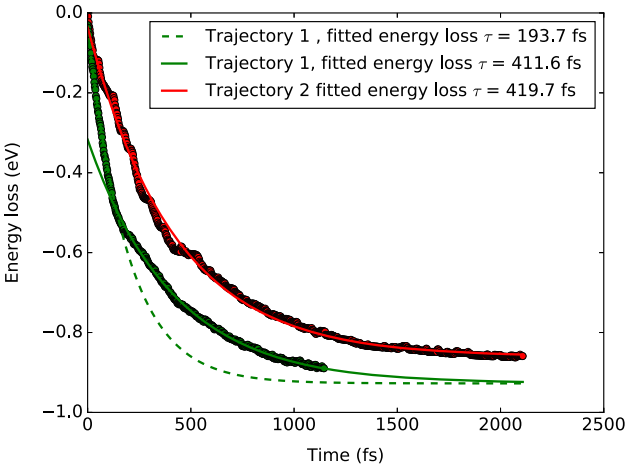

Fig. 8 Energy loss as a function of time for two characteristic trajectories, the green one leading to direct absorption and the red one to adsorption. The dotted and continuous lines are exponential fittings (see text)

the surface, as well as multiple-timescale energy loss behaviors. Preliminary results with a statistics over 64 trajectories yield 25% reflection, 50% adsorption and 25% absorption.

In future works achieving larger statistics, it would be interesting to analyze in more details the locations of the adsorbed and absorbed hydrogen atoms, as well as to study the effect of varying incidence angles and energies, and finally compare with H-Ag(111). The H–Ag(100) system was motivated by the experimental studies of Kolovos-Vellianitis and Küppers [25] who did not evidence H subsurface insertion with Ag(111) whereas subsurface insertion could become much larger than adsorption on the surface at the highest H exposures with Ag(100). Furthermore, at these high exposures, a surface reconstruction could be evidenced for H and yet not for D, which then represents a huge isotopic effect. In addition, the above authors estimated large cross-sections of abstraction reactions, namely molecular hydrogen recombinations between an incoming hydrogen atom and an adsorbed one, for H reacting with D/Ag(100) and D/Ag(111) as a function of coverage [25]. The present work represents the first step through the development of an accurate and an efficient theoretical description of tens of scattering or diffusing hydrogen atoms with dissipative friction dynamics as well as of hundreds of vibrating and/or relaxing silver atoms at the least, in order to address those challenging experimental results.

Acknowledgements This study has been supported through the EUR grant NanoX n° ANR-17-EURE-0009 in the framework of the "Programme des Investissements d'Avenir". This work was performed using HPC resources from CALMIP (Grant 2020-P18019). We thank Bruno Lepetit at LCAR for helpful discussions and suggestions.

Data availability No data associated in the manuscript.

References

1. M. Rapacioli, T. Heine, L. Dontot, M. Yusef Buey, N. Tarrat, F. Spiegelman, F. Louisnard, C. Marti, J. Cuny, M. Morinière, C. Dubosq, S. Patchkovskii, J. Frenzel, E. Michoulier, H. Duarte, L. Zchekhov, D. Salahub, 2023 deMonNano experiment, http://demon-nano.ups-tlse.fr/, (2023)
2. S.A. Adelman, J.D. Doll, J. Chem. Phys. **64**, 2375–2388 (1976)
3. T.A. Alrebdi, H. Souissi, F.H. Alkallas, F. Aouani, Ab initio adiabatic study of the agh system. Sci. Rep. **11**, 8277 (2021)
4. B. Aradi, B. Hourahine, Th. Frauenheim, Dftb+, a sparse matrix-based implementation of the dftb method. J. Phys. Chem. A **111**(26), 5678–5684 (2007). (**PMID: 17567110**)
5. M. Askerka, R.J. Maurer, V.S. Batista, J.C. Tully, Role of tensorial electronic friction in energy transfer at metal surfaces. Phys. Rev. Lett. **116**, 217601 (2016)
6. B.B. Zhou, E. Carter, First principles local pseudopotential for silver: towards orbital-free density-functional theory for transition metals. J. Chem. Phys. **122**, 184108 (2005)
7. M. Blanco-Rey, J.I. Juaristi, R. Díez Muiño, H.F. Busnengo, G.J. Kroes, M. Alducin, Electronic friction dominates hydrogen hot-atom relaxation on pd(100). Phys. Rev. Lett. **112**(10), 103203 (2014)
8. P.E. Blöchl, Projector augmented-wave method. Phys. Rev. B **50**(24), 17953–17979 (1994)
9. J. Cuny, N. Tarrat, F. Spiegelman, A. Huguenot, M. Rapacioli, Density-functional tight-binding approach for metal clusters, nanoparticles, surfaces and bulk application to silver and gold. J. Phys. Condens. Matter **30**(30), 303001 (2018)
10. J. Donohue, *The Structures of the Elements* (1974)
11. P.M. Echenique, R.M. Nieminen, R.H. Ritchie, Density functional calculation of stopping power of an electron gas for slow ions. Solid State Commun. **37**(10), 779–781 (1981)
12. M. Elstner, D. Porezag, G. Jungnickel, J. Elsner, M. Haugk, T. Frauenheim, S. Suhai, G. Seifert, Self-consistent-charge density-functional tight-binding method for simulations of complex materials properties. Phys. Rev. B **58**, 7260–7268 (1998)
13. P. Ferrin, S. Kandoi, A.U. Nilekar, M. Mavrikakis, Hydrogen adsorption, absorption and diffusion on and in transition metal surfaces: a DFT study. Surf. Sci. **606**(7), 679–689 (2012)
14. M. Forsblom, M. Persson, Vibrational lifetimes of cyanide and carbon monoxide on noble and transition metal surfaces. J. Chem. Phys. **127**(15), 154303 (2007)
15. T. Frauenheim, G. Seifert, M. Elsterner, Z. Hajnal, G. Jungnickel, D. Porezag, S. Suhai, R. Scholz, A self-consistent charge density-functional based tight-binding method for predictive materials simulations in physics, chemistry and biology. Phys. Stat. Solidi (b) **217**, 41–62 (2000)
16. T. Frauenheim, G. Seifert, M. Elstner, T. Niehaus, C. Köhler, M. Amkreutz, M. Sternberg, Z. Hajnal, A. Di Carlo, S. Suhai, Atomistic simulations of complex materials: ground-state and excited-state properties. J. Phys. Cond. Mat. **14**, 3015 (2002)
17. M. Head-Gordon, J.C. Tully, Vibrational relaxation on metal surfaces: molecular-orbital theory and application to co/cu(100). J. Chem. Phys. **96**(5), 3939–3949 (1992)
18. Martin Head-Gordon, John C. Tully, Molecular dynamics with electronic frictions. J. Chem. Phys. **103**(23), 10137–10145 (1995)
19. B. Hellsing, M. Persson, Electronic damping of atomic and molecular vibrations at metal surfaces. Phys. Scr. **29**(4), 360 (1984)
20. N. Hertl, A. Kandratsenka, A.M. Wodtke, Effective medium theory for bcc metals: electronically non-adiabatic h atom scattering in full dimensions. Phys. Chem. Chem. Phys. **24**, 8738–8748 (2022)
21. N. Hertl, R. Martin-Barrios, O. Galparsoro, P. Larrégaray, D.J. Auerbach, D. Schwarzer, A.M. Wodtke, A. Kandratsenka, Random force in molecular dynamics with electronic friction. J. Phys. Chem. C **125**(26), 14468–14473 (2021)
22. K.P. Huber, G. Herzberg, Constants of doiatomic molecule's. Mol. Spectra Mol. Struct. **4**, 146–291 (1979)
23. P. Janthon, S.A. Luo, S.M. Kozlov, F. Viñes, J. Limtrakul, D.G. Truhlar, F. Illas, Bulk properties of transition metals: a challenge for the design of universal density functionals. J. Chem. Theory Comput. **10**, 3832–3839 (2014)
24. J.I. Juaristi, M. Alducin, R. Díez Muiño, H.F. Busnengo, A. Salin, Role of electron-hole pair excitations in the dissociative adsorption of diatomic molecules on metal surfaces. Phys. Rev. Lett. **100**, 116102 (2008)
25. D. Kolovos-Vellianitis, J. Küppers, Abstraction of D on Ag(100) and Ag(111) surfaces by gaseous H atoms: the role of electron-hole excitations in hot atom reactions and the transition to Eley-Rideal kinetics. Surf. Sci. **548**(1), 67–74 (2004)
26. P. Koskinen, V. Makinen, Density-functional tight-binding for beginners. Comput. Mat. Sc. **47**(1), 237–253 (2009)
27. G. Kresse, J. Furthmüller, Efficiency of ab-initio total energy calculations for metals and semiconductors using a plane-wave basis set. Comput. Mater. Sci. **6**(1), 15–50 (1996)
28. G. Kresse, J. Furthmüller, Efficient iterative schemes for ab initio total-energy calculations using a plane-wave basis set. Phys. Rev. B **54**(16), 11169–11186 (1996)
29. G. Kresse, J. Hafner, Ab initio molecular dynamics for liquid metals. Phys. Rev. B **47**(1), 558–561 (1993)
30. G. Kresse, D. Joubert, From ultrasoft pseudopotentials to the projector augmented-wave method. Phys. Rev. B **59**(3), 1758–1775 (1999)
31. R. Martin-Barrios, N. Hertl, O. Galparsoro, A. Kandratsenka, A.M. Wodtke, P. Larrégaray, H atom scattering from w(110): a benchmark for molecular dynamics with electronic friction. Phys. Chem. Chem. Phys. **24**(35), 20813–20819 (2022)
32. R.J. Maurer, M. Askerka, V.S. Batista, J.C. Tully, Ab initio tensorial electronic friction for molecules on metal surfaces: nonadiabatic vibrational relaxation. Phys. Rev. B **94**, 115432 (2016)
33. L.F.L. Oliveira, N. Tarrat, J. Cuny, J. Morillo, D. Lemoine, F. Spiegelman, M. Rapacioli, Benchmarking density functional based tight-binding for silver and gold materials: from small clusters to bulk. J. Phys. Chem. A **120**(42), 8469–8483 (2016)

34. J.P. Perdew, K. Burke, M. Ernzerhof, Generalized gradient approximation made simple. Phys. Rev. Lett. **77**(18), 3865–3868 (1996)
35. J.P. Perdew, K. Burke, M. Ernzerhof, Generalized gradient approximation made simple [phys. rev. lett. 77, 3865 (1996)]. Phys. Rev. Lett. **78**(7), 1396–1396 (1997)
36. D. Porezag, T. Frauenheim, T. Köhler, G. Seifert, R. Kaschner, Phys. Rev. B **51**, 12947–12957 (1995)
37. M. Rapacioli, N. Tarrat, Periodic dftb for supported clusters: implementation and application on benzene dimers deposited on graphene. Computation **10**(3), 39 (2022)
38. S.P. Rittmeyer, J. Meyer, J.I. Juaristi, K. Reuter, Electronic friction-based vibrational lifetimes of molecular adsorbates: beyond the independent-atom approximation. Phys. Rev. Lett. **115**(4), 046102 (2015)
39. G. Seifert, D. Porezag, T. Frauenheim, Int. J. Quant. Chem. **58**, 185–192 (1996)
40. F. Spiegelman, N. Tarrat, J. Cuny, L. Dontot, E. Posenitskiy, C. Martí, A. Simon, M. Rapacioli, Density-functional tight-binding: basic concepts and applications to molecules and clusters. Adv. Phys.: X **5**(1), 1710252 (2020)
41. B. Szűcs, Z. Hajnal, R. Scholz, S. Sanna, Th. Frauenheim, Theoretical study of the adsorption of a ptcda monolayer on s-passivated gaas(1 0 0). Appl. Surf. Sci. **234**(1–4), 173–177 (2004)
42. J.C. Tully, J. Chem. Phys. **73**, 6333–42 (1980)
43. J.C. Tully, Molecular dynamics with electronic transitions. J. Chem. Phys. **93**(2), 1061–1071 (1990)
44. H.A. Witek, D.G. Fedorov, K. Hirao, A. Viel, P.-O. Widmark, Theoretical study of the unusual potential energy curve of the state of agh. J. Chem. Phys. **116**(19), 8396–8406 (2002)
45. H.A. Witek, T. Nakijima, K. Hirao, Relativistic and correlated all-electron calculations on the ground and excited states of agh and auh. J. Chem. Phys. **113**(18), 8015–8025 (2000)